MINERALOGY OF THE COMPLEX REFRACTORY METAL NUGGETS IN B1 TYPE CAI FROM CV3-CHONDRITE NORTHWEST AFRICA 12590. Ksenia A. Konovalova[1], Pavel Yu. Plechov[1], Konstantin D. Litasov[1,2], Vasily D. Shcherbakov[3], Sergey P. Vasiliev[1], [1]Fersman Mineralogical Museum, Russian Academy of Sciences, Moscow, 119071, Russia (pplechov@gmail.com), [2]Vereshchagin Institute for High Pressure Physics, Russian Academy of Sciences, Moscow, 108840, Russia, [3]Department of Geology, Moscow State University, Moscow, 119992, Russia

Introduction: Ca-Al-inclusions are the oldest objects in the solar system, which contain minerals, such as spinel, melilite, hibonite, and perovskite, presumably condensed from a cooling gas of the solar nebula [1]. They often contain fremdlinge and refractory metal nuggets (RMN), that are enriched by siderophile elements such as PGE, Mo, and W [2-3].

Three major groups of hypotheses have been proposed to explain the origin of RMN: (1) condensation from the solar nebula or stellar environments, which is supported by data from type A CAI and studies of presolar grains [4-7]; (2) precipitation from CAI melt, which is very likely for type B CAI [8-9], or (3) secondary processes in the parent bodies or nebulae, which may be applicable for PMNs in fremdlinge and RMN of complex composition [10-11].

Here we report the detailed data on RMNs from B1 type CAI in new CV3 chondrite Northwest Africa (NWA) 12590 [12], which revealed the complex inner structure and multiple origin.

Methods: The mineral composition in B1 type CAI from polished plates of NWA 12590 was obtained by Oxford X-Max^N EDS spectrometer installed on the JEOL JSM-6480 SEM.

Results and Discussion: Rounded RMN up to 20 μm in size are included into melilite, Ti-clinopyroxene, and spinel. Fe-Ni-bearing inclusions may have an irregular shape and larger sizes up to 50-60 μm (Figs. 1-2). Most RMN have a heterogenous microstructure and typically include Fe-Ni bearing part (hexaferrum and garutiite [13]) and hexamolybdenum enriched in PGE elements. Besides, some RMN contain non-metallic phases, such as oxides represented by scheelite, kamiokite ($Fe_2Mo_3O_8$), and fersmite ($CaNb_2O_6$) and molybdenum carbide (Figs. 1-2).

The composition of hexaferrum, garutiite, and hexamolybdenum vary widely (Table 1). Hexaferrum and garutiite are enriched by Ir and Pt. Mo-bearing phases are enriched by Ru, Os, Ir, W, and Re and can be classified by predominant constituent element to Mo-, Ru-, Os-, and Ir-bearing varieties (and also to Fe, Table 1).

Osmium and Ruthenium has hexagonal crystal structures. Thus, it is possible to name hexaosmium (H-Os) and hexaruthenium (H-Ru) as simply osmium and ruthenium. However, to emphasize specific composition and type of origin "hexa-" may be important. Pure Molybdenum and Iridium (also Fe and Ni) have cubic crystal structure, however, with an

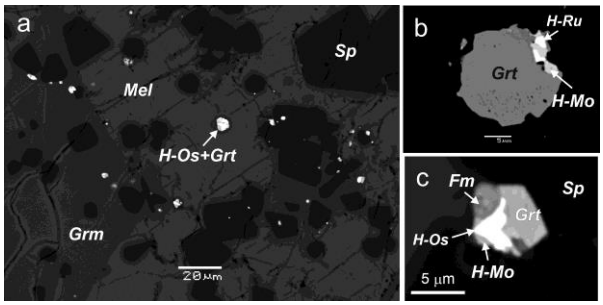

Fig. 1. BSE images of type B1 CAI from NWA 12590 CV3 chondrite with abundant refractory metal nuggets (a) and their examples (b-c). Grt – Garutiite (Hexanickel), H-Mo – Hexamolybdenum, H-Ru – Hexaruthenium, H-Os – Hexaosmium, Fm – Fersmite ($CaNb_2O_6$), Grm – Grossmanite-diopside, Sp – Spinel, Mel – Melilite.

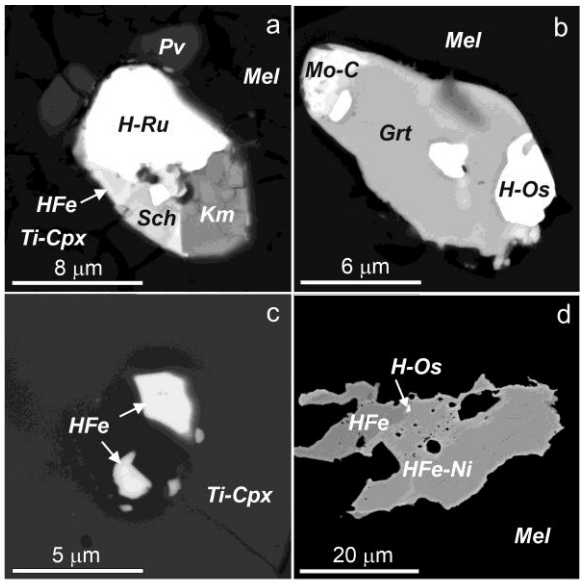

Fig. 2. (a-d). BSE images of metallic nuggets from CAI in NWA 12590. HFe – Hexaferrum, HFe-Ni – Ni-bearing hexaferrum, Sch – Scheelite, Km – Kamiokite ($Fe_2Mo_3O_8$), Mo-C – Mo-carbide or oxycarbide, Pv –

Perovskite, Ti-Cpx – Ti-clinopyroxene. See Fig. 1 for other abbreviations.

Table 1. Representative hexagonal metallic phase compositions (wt.%) from refractory metal nuggets.

Min.	HFe	HFe	Grt	HMo	HRu	HOs	HIr
Fe	**33.6**	**43.8**	32.8	9.01	9.73	2.61	4.03
Co	-	0.94	1.7	0.93	-	-	0.28
Ni	1.45	24.7	**53.4**	11.4	1.23	1.49	3.18
Mo	31.7	-	-	**24.2**	19.5	13.5	15.5
Ru	12.9	7.65	-	23.5	**26.9**	8.37	5.37
Rh	1.13	1.17	-	-	-	-	-
W	-	-	-	-	-	-	6.35
Re	2.94	-	-	-	-	4.47	2.27
Os	12.8	3.17		16.2	15.9	**43.4**	28.5
Ir	2.76	3.29	7.92	13.1	23.0	24.9	**33.0**
Pt	0.59	11.7	2.87	1.64	1.87	-	1.13
Sum	99.8	96.4	98.7	99.9	98.1	98.8	99.5

HIr – hexairidium. See Figs. 1-2 for other abbreviations. "-" – below detection limit.

addition of the significant amount of impurities they become hexagonal and "hexa-" is essential [11, 14].

Scheelite coexists with H-Fe, H-Ru, and kamiokite and contains a significant amount of SrO = 5.2 wt.% and MoO_3 = 10.9 wt.%. Scheelite-powellite solid solution grains are common in fremdlinge from Allende chondrite [15]. Kamiokite contains minor impurities of MgO = 2.5 wt.% and CaO = 1.0 wt.%. Kamiokite and majindeite ($Mg_2Mo_3O_8$) were also observed in Allende [16-17].

Fersmite was described in meteorites for the first time. It coexists with H-Mo, H-Os, and garutiite (Fig.1c) and has a complex composition with a range of impurities (Ni, Fe, Ti, Ir, W, and REEs). The approximate formula can be written as $(Ca_{0.72}Mg_{0.28})(Nb_{1.9}Mo_{0.1})_2O_6$. We should note that REE- and Th-bearing pyrochlore-type minerals and Ca-niobates were noticed in Allende meteorite [18-19].

Mo-carbide or oxycarbide coexists with garutiite and H-Os and contains (wt.%) Mo = 81-84, W = 2.0, and O = 6.3. It has a pronounced carbon peak in EDS spectra and a total deficit of about 6 wt.%. Thus, this phase may correspond to $Mo_2C_{1-x}O_x$. We found carbide inclusion in RMN for the first time, but this yet to be additionally confirmed. Oxides, sulfides, and carbides in RMN can be formed by the secondary process. Mo and W are easy to oxidize and their abundance in RMN may become lower by oxidation. The presence of carbon in RMN was observed in [20], whereas possibility of Mo-carbide formation was shown in the melting experiments on RMN formation in [8].

References: [1] MacPherson G. J. (2014) In: *Treatise on Geochemistry (2nd ed.), v.1, Meteorites, Comets and Planets*, Elsevier, p. 139-179. [2] Wark D. A. and Lovering J. F. (1976) *LPSC VII*, #1317. [3] El Goresy A. et.al. (1978) *LPSC IX*, #1100. [4] Berg T. et al. (2009) *Astrophys. J. 702*, L172–L176. [5] Croat T. K. et al. (2013) *MAPS 48*, 686–699. [6] Daly L. et al. (2017) *GCA 216*, 61-81. [7] Pan M. (2020) *Icarus 350*, 113851. [8] Schwander D. et al. (2015) *MAPS 50*, 893-903. [9] Rudraswami N. G. et al. (2014) *GCA 131*, 247-266. [10] Blum J. D. et al. (1988) *Nature 331*, 405-409. [11] Daly L. et al. (2017) *GCA 216*, 42-60. [12] Konovalova K. A. et al. (2021) *LPSC 52*, #1517. [13] McDonald A. M. et al. (2010) *Eur. J. Mineral. 22*, 293-304. [14] Harries D. et al. (2012) *MAPS 47*, 2148-2159. [15] Bischoff A. and Palme H. (1987) *GCA 51*, 2733-2748. [16] Ma C. et al. (2014) *Am. Min. 99*, 198-205. [17] Ma C. and Beckett J. R. (2016) *Am. Min. 101*, 1161-1170. [18] Lovering J. F. et al. (1979) *LPSC X*, 745-747. [19] Schwander D. et al. (2015) *GCA 168*, 70-87. [20] Schwander D. et al. (2014) *MAPS 49*, 1888-1901.